MicroRNA-129 plays a protective role in sepsis-induced acute lung injury through the suppression of pulmonary inflammation via the modulation of the TAK1/NF-κB pathway

WENJIAN YAO, LEI XU, XIANGBO JIA, SAISAI LI and LI WEI

Department of Thoracic Surgery, Henan Provincial People's Hospital, People's Hospital of Zhengzhou University, School of Clinical Medicine, Henan University, Zhengzhou, Henan 450003, P.R. China

Received September 26, 2020; Accepted May 7, 2021

DOI: 10.3892/ijmm.2021.4972

Abstract. Excessive inflammatory response and apoptosis play key roles in the pathogenic mechanisms of sepsis-induced acute lung injury (ALI); however, the molecular pathways linked to ALI pathogenesis remain unclear. Recently, microRNAs (miRNAs/miRs) have emerged as important regulators of inflammation and apoptosis in sepsis-induced ALI; however, the exact regulatory mechanisms of miRNAs remain poorly understood. In the present study, the gene microarray dataset GSE133733 obtained from the Gene Expression Omnibus database was analyzed and a total of 38 differentially regulated miRNAs were identified, including 17 upregulated miRNAs and 21 downregulated miRNAs, in mice with lipopolysaccharide (LPS)-induced ALI, in comparison to the normal control mice. miR-129 was found to be the most significant miRNA, among the identified miRNAs. The upregulation of miR-129 markedly alleviated LPS-induced lung injury, as indicated by the decrease in lung permeability in and the wet-to-dry lung weight ratio, as well as the improved survival rate of mice with ALI administered miR-129 mimic. Moreover, the upregulation of miR-129 reduced pulmonary inflammation and apoptosis in mice with ALI. Of note, transforming growth factor activated kinase-1 (TAK1), a well-known regulator of the nuclear factor-κB (NF-κB) pathway, was directly targeted by miR-129 in RAW 264.7 cells. More importantly, miR-129 upregulation impeded the LPS-induced activation of the TAK1/NF-κB signaling pathway, as illustrated by the suppression of the nuclear phosphorylated-p65, p-IκB-α and p-IKKβ expression levels. Collectively, the findings of the present study indicate that miR-129 protects mice against sepsis-induced ALI by suppressing pulmonary inflammation and apoptosis through the regulation of the TAK1/NF-κB signaling pathway. This introduces the basis for future research concerning the application of miR-129 and its targets for the treatment of ALI.

Correspondence to: Dr Li Wei, Department of Thoracic Surgery, Henan Provincial People's Hospital, People's Hospital of Zhengzhou University, School of Clinical Medicine, Henan University, 7 Weiwu Road, Zhengzhou, Henan 450003, P.R. China
E-mail: liweilw03@163.com

Key words: acute lung injury, microRNA-129, inflammatory response, TAK1/NF-κB pathway

Introduction

Sepsis, which is a highly complex syndrome, is one of the leading causes of mortality in patients suffering from trauma, burns and critical surgery (1). Furthermore, severe sepsis develops into acute lung injury (ALI) in 50% of patients. In septic conditions, the excessive inflammatory response and apoptosis leads to the disruption of alveolar epithelial cells, an increase in epithelial permeability, and the influx of edema fluid into the alveolar space, finally leading to ALI (2). Thus, the control of aberrant inflammation and apoptosis contributes substantially toward improving the prognosis of patients with ALI. However, there is no current effective therapeutic approach for sepsis, and its treatment involves significant healthcare costs (3).

The overwhelming inflammatory response that occurs in ALI can lead to the release of a large number of pro-inflammatory cytokines in the lungs, such as interleukin (IL)-6, tumor necrosis factor-α (TNF-α) and IL-1β, that ultimately lead to alveolar epithelial cell death (4,5). However, the factors that play a role in the transmission of inflammatory signals associated with ALI have not yet been fully elucidated. Nuclear factor-κB (NF-κB) has been recognized as an important inflammatory mediator in a number of diseases, including lupus nephritis, cancers (6,7) and ALI (8,9). Once NF-κB dimers are activated in response to certain stimuli, they enter the nucleus and lead to inflammatory cytokine expression. It has been reported that the degree of activation of NF-κB is associated with disease complications and a more severe outcome in patients with ALI (10,11). Transforming growth factor-β (TGF-β)-activated kinase 1 (TAK1, also known as MAP3K7) is a serine/threonine protein kinase that is critically involved in the activation of NF-κB. Activated TAK1 can induce the phosphorylation of inhibitor of IκB kinase (IKK) and lead to IKK-induced NF-κB activation, which then leads to the synthesis and release of pro-inflammatory mediators (12). All these findings indicate

that the targeting of TAK1/NF-κB pathway may provide novel treatment strategies for patients with ALI.

MicroRNAs (miRNAs/miRs) are a family of short, small, non-coding RNAs that negatively regulate target gene expression through either translation repression or RNA degradation (13). Increasing evidence has demonstrated that miRNAs are effective regulators of the inflammatory response and apoptosis in various types of organ injuries (14-16). For example, Li *et al* (17) found that an increase in miR-129 levels leads to the amelioration of neuroinflammation and damage to the blood-spinal cord barrier after ischemia-reperfusion (I/R), via the inhibition of high mobility group box-1 (HMGB1) and the TLR3-cytokine pathway. miR-129 was also reported to alleviate nerve injury and inflammatory response in Alzheimer's disease via the downregulation of SOX6 (18). Furthermore, Chen *et al* (19) demonstrated the protective effect of miR-129 on myocardial I/R injury through the suppression of cardiomyocyte apoptosis via targeting HMGB1 in rats. Based on these previous findings, it is possible that miR-129 plays a role in inflammation and apoptosis in ALI. However, the role of miR-129 in the pathogenesis of ALI is largely unknown.

The aim of the present study was to investigate the role of miRNAs in the pathogenesis of ALI. To this end, several differentially expressed miRNAs deposited in a public dataset, namely, the Gene Expression Omnibus (GEO) database (GSE133733), were evaluated concerning their potential role in ALI. Based on an analysis of these miRNAs, miR-129 was selected for further analysis. Using a mouse model of ALI, the functional role and underlying mechanisms of miR-129 were investigated. The findings presented herein may prove useful for the development of novel research strategies for the molecular therapeutic targeting of ALI.

Materials and methods

Animals and treatment. Male BALB/c mice (age, 6 weeks; weight, 18-22 g) were purchased from Shanghai SLAC Laboratory Animal Co., Ltd. All mice were housed under standard conditions (12-h light-dark cycle at 25-27˚C and ~40% humidity) with free access to food and water.

The mice were randomly divided into four groups (10 mice per group) as follows: i) The control group: 1.5 mg/kg normal saline (NS) was administered; ii) lipopolysaccharide (LPS) group: 0.2 ml of LPS (10 mg/kg, *Escherichia coli* 055:B5; Sigma-Aldrich; Merck KGaA) was intravenously administered via the tail vein; iii) LPS + agomir-129 group; and iv) LPS + agomir negative control (NC) group. In the mice in the agomir-129/agomir-NC group, in addition to LPS, 0.2 ml agomir-129/agomir-NC (8 mg/kg) was intravenously administered via the tail vein (20). Agomir-129 or agomir-NC were injected intravenously via the tail vein every third day until ALI was induced. Pentobarbital sodium (50 mg/kg, intraperitoneal injection) was used for anesthesia before each operation, and all efforts were made to minimize animal suffering. No mice were found dead during the anesthesia process. If an animal reached the defined humane endpoints [a >15% body weight loss in 1-2 days or an overall >20% loss in body weight or displayed obvious signs of suffering (lethargy, squinted eyes, dehydration or hunched back), it was humanely euthanized. Sacrifice was performed by an intraperitoneal injection of pentobarbital sodium (50 mg/kg) followed by cervical dislocation, and the death of the mice was confirmed by the cessation of respiration and heartbeat (21). In the survival experiment, the mice were observed for 7 days after the LPS injection, while other mice were observed for 3 days after the LPS injection. All mice were humanely sacrificed when they reached the humane endpoint or the set experimental endpoint. The lungs were then excised, intact. Subsequently, the trachea was lavaged with 1 ml of sterile ice-cold PBS and bronchoalveolar lavage fluid (BALF) was collected. BALF was pooled and centrifuged at 200 x g for 10 min at 4˚C, and the harvested supernatant was stored at -80˚C until mediator analysis.

In addition, the survival experiments were performed in 4 groups of mice (n=10/group) (LPS, Control, LPS + agomir-129, LPS + agomir-NC). The survival rate was defined from 0 to 7 days following treatment and analyzed with the Kaplan-Meier survival analysis and the log rank test. All animal experiments were approved by the Animal Care and Use Committee of Henan Provincial People's Hospital (approval no. 2019-00112).

miRNA expression profile data from GEO. miRNA data (accession no. GSE133733) were downloaded from open microarray datasets, deposited in NCBI's GEO database (http://www.ncbi.nlm.nih.gov/geo/). The miRNA array expression data were analyzed with the Qlucore Omics Explorer (QOE 3.1) bioinformatics software (http://www.qlucore.com/).

Cell culture and transfection. RAW 264.7 cells (cat. no. ATCC® TIB-71) were obtained from ATCC and cultured in DMEM/F12 supplemented with 10% FBS (Abcam) at 37˚C and in a 5% CO_2 atmosphere. RAW264.7 cells ($2x10^5$ cells) were seeded in a 6-well plate and transfected with 100 nM of miR-129 mimics/inhibitor at 37˚C for 48 h using Lipofectamine® 2000 (Invitrogen; Thermo Fisher Scientific, Inc.). miR-129 mimic/inhibitor and their NC oligonucleotides (NC mimic or NC inhibitor) were obtained from Shanghai GenePharma Co., Ltd. The sequences were as follows: miR-129 mimic, 3'-CUUUUUGCGGUCUGGGCUUGC-5'; miR-129 inhibitor, 3'-GCAAGCCCAGACCGCAAAAAG-5'; mimic NC, 5'-UUUGUACUACACAAAAGUACUG-3'; inhibitor NC, 5'-UUCUCCGAACGUGUCACGUTT-3'. The cells were harvested at 48 h following transfection for testing.

Transfection of pcDNA-TAK1 and si-TAK1. A series of ALI cell models have been established to simulate the status of ALI caused by diverse pathogeneses. The human type II lung epithelial A549 cell line is usually used to establish cell apoptosis models in LPS-induced ALI (22,23). Among these, RAW 264.7 macrophages are usually used to establish cell inflammation responses models in LPS-induced ALI (24,25). Therefore, RAW cells were selected for use in *ex vivo* experiments as the focus of the present study was on the inflammatory responses in ALI. For this purpose, RAW 264.7 cells were co-transfected with miR-129 mimics (100 nmol/l), pcDNA-TAK1 (2 μg), or si-TAK1 (100 nmol/l) for 48 h using Lipofectamine 3000® (Invitrogen; Thermo Fisher Scientific, Inc.) at 37˚C in 5% CO_2, followed by LPS stimulation (100 ng/ml) for a further 6 h, as previously described (26). Subsequently, they were cultured in complete medium for 48 h, in order to perform the subsequent experiments. A TAK1 expression vector was

constructed through the insertion of the full sequence of TAK1 into the pcDNA 3.1 vector (Invitrogen; Thermo Fisher Scientific, Inc.). Specific small interfering RNAs (siRNAs) for TAK1 (5'-CATCCAGTGCCAAGCAGCTCATATT-3') and si-Scramble (5'-CATGAGTCCAACGGATCACTCCATT-3') were purchased from Shanghai GenePharma Co., Ltd. RAW 264.7 cells co-transfected with the pcDNA-vector and si-Scramble were used as a control group. Agomir-129 and agomir-NC were synthesized by GenePharma Co., Ltd. The agomiR-129 and agomiR-NC, whose sequence was the same as the miR-129 mimics and mimics NC, were modified with methylation, cholesterol addition and thiophosphorylation, in order to improve the stability and transfection efficiency and to simulate miRNA activity in the animal body (27).

Reverse transcription-quantitative PCR (RT-qPCR) analysis. Total RNA was isolated from the lung tissues using the RNeasy Mini kit (Qiagen GmbH). Reverse transcripts of miR-129 and TAK1 were synthesized using the MicroRNA Reverse Transcription kit (Thermo Fisher Scientific, Inc.) and the PrimeScript RT reagent kit (Takara Bio, Inc.), respectively. miR-129 and TAK1 expression was measured with SYBR-Green (Beijing Solarbio Science & Technology Co., Ltd.) on a Light Cycler instrument (Bio-Rad Laboratories, Inc.). The following primers were used for RT-qPCR analysis: miR-129 forward, 5'-GTTGGGGAGATTTAGTTTGTT-3' and reverse, 5'-CCTACTCCAATTCCCCCTATAATAC-3'; U6 forward, 5'-CTCGCTTCGGCAGCACA-3' and reverse, 5'-AACGCTTCACGAATTTGCGT-3'; TAK1 forward, 5'-GATATCCTGTCGACAGCCTCCGC-3' and reverse, 5'-AACGTAACGGGCCCAGAGAA-3'; GAPDH forward, 5'-GTGGTGAAGACGCCAGTGGA-3' and reverse, 5'-CGAGCCACATCGCTCAGACA-3'. The thermocycling conditions were as follows: 50˚C for 2 min and 95˚C for 10 min, followed by 40 cycles of 95˚C for 15 sec and 60˚C for 10 min. Relative miRNA expression was analyzed using the $2^{-\Delta\Delta Cq}$ method (28).

Lung histology. Mouse lungs from all groups were fixed with 10% formalin and micro-sectioned to a thickness of 5 μm using a Leica SM2010R microtome (Leica Microsystems, Inc.). The tissues were embedded in paraffin and then subjected to hematoxylin and eosin (H&E) staining. Images were viewed and captured by a Nikon E-800M microscope (Nikon Corporation) at x200 magnification. Inflammatory cell infiltration, bleeding and interstitial and alveolar edema were observed under a light microscope, according to the following lung injury score: 0, normal pulmonary appearance; 1, slight injury, mild interstitial congestion and neutrophil leukocyte infiltrations; 2, moderate injury: Moderate interstitial congestion and neutrophil leukocyte infiltrations; 3, severe injury, perivascular edema formation, partial leukocyte infiltration, moderate neutrophil leukocyte infiltration; 4, very severe histological injury: Severe destruction of the lung architecture and massive neutrophil leukocyte infiltration.

Lung permeability. The Evans blue (EB) (Sigma-Aldrich; Merck KGaA) dye extravasation method was used to assess pulmonary permeability, as previously described (29). The dye concentration was reported as the absorbance relative to the weight of dry lung tissue (μg/100 mg dry tissue).

Lung wet/dry ratio. Following a 72-h LPS challenge, the mice were sacrificed. The lungs were excised, and the right lungs were weighed and dried in an incubator at 55˚C. After 60 h, the lungs were weighed again to calculate the wet-to-dry (W/D) ratio.

Measurement of pro-inflammatory cytokine levels. Murine cytokine-specific Quantikine ELISA kits (R&D Systems Europe, Ltd.) were used to detect the IL-6, IL-1β, TNF-α, Cxcl2, JE (the murine homolog of human CCL2) and KC (the murine homolog of human IL-8) levels in BALF, as previously described (14).

TUNEL staining. The lung tissue sections were deparaffinized with xylene, rehydrated with ethanol at graded concentrations of 70-100% (v/v) and washed with water. The sections were then treated with 100 μl proteinase K (20 μg/ml, Roche Diagnostics) for 15 min, at room temperature. After the sections were washed three times with PBS, they were stained with prepared terminal deoxynucleotidyl transferase-mediated dUTP-biotin nick-end labeling (TUNEL) solution, using the *in situ* Cell Death Detection kit (Roche Diagnostics). Cell quantification was performed under an inverted fluorescence microscope (DP73; Olympus Corporation) at x200 magnification. TUNEL-positive cells were counted in three fields of view per section.

Bioinformatics analysis. The miRNA target prediction tools PicTar version 2007 (https://pictar.mdc-berlin.de/) and TargetScan Release 7.0 (http://targetscan.org/) were used to search for putative targets of miR-153.

Luciferase assay. The 3'-UTR of TAK1 and its mutated sequence were inserted into the pGL3 control vector (Promega Corporation) to construct the wild-type (wt) TAK1-3'-UTR vector and mutant TAK1-3'-UTR vector, respectively. RAW 264.7 cells were seeded in 24-well plates ($5.0x10^5$/well) and were transfected with either the wild-type or mutant reporter vector (2 μg), combined with the miR-129 mimics/inhibitor (100 nM), using Lipofectamine 2000® (Invitrogen, Thermo Fisher Scientific Inc.). The *Renilla* luciferase expression vector pRL-TK (Promega Corporation) was employed as the reference. At 48 h post-transfection, luciferase activity was detected using the dual luciferase reporter kit (Beyotime Institute of Biotechnology).

Immunohistochemistry. The expression of cleaved caspase-3, TAK1 and p-p65 in the lung sections was evaluated by immunohistochemical staining, as previously described (30), with the following primary antibodies diluted to 1:200: Cleaved caspase-3 (cat no. 9664, Cell Signaling Technology, Inc.), TAK1 (cat no. 5206, Cell Signaling Technology, Inc.), and p-p65 (cat no. 3036, Cell Signaling Technology, Inc.). Samples were photographed under a Leica DMD 108 light microscope. Immunohistochemical staining was independently evaluated by two observers, and the immunohistochemistry images of lung tissue samples were scored as previously described (31).

Western blot analysis. Total protein was extracted using the RIPA buffer. The extraction and isolation of nuclear and

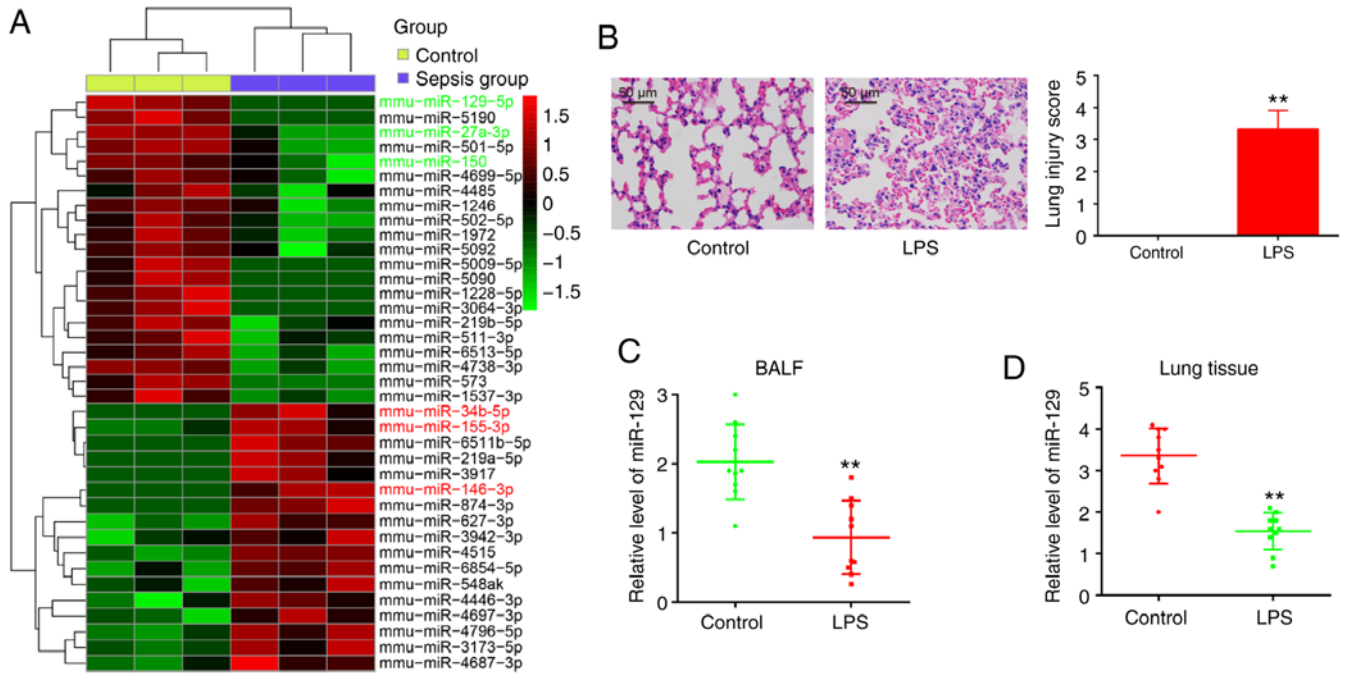

Figure 1. Downregulation of miR-129 in mice with LPS-induced ALI. Mice (n=10 each) were treated with 0.2 ml LPS (10 mg/kg, *Escherichia coli* 055:B5) or normal saline and total RNA were isolated from their lungs at 72 h following LPS administration. (A) Heatmap of the miRNA profiles demonstrated the miRNAs with significantly different expression between the control mice and mice with LPS-induced ALI. (B) H&E-stained sections of lung tissue from control and LPS-treated mice (x200 magnification) revealed damage to the lung architecture in the LPS-induced ALI group. (C and D) RT-qPCR analysis of the lung tissues and BALF of mice challenged with LPS (10 mice per group) revealed that miR-129 expression was significantly reduced. Data represent the mean ± SD of three independent experiments. **P<0.01 vs. the control group. LPS, lipopolysaccharide; ALI, acute lung injury; BALF, bronchoalveolar lavage fluid.

cytoplasmic proteins were performed with the Cytoplasmic and Nuclear Protein Extraction kit (cat no. 78833, Thermo Fisher Scientific, Inc.), according to the manufacturer's instructions. The protein concentration was determined using the bicinchoninic acid assay (Pierce, Thermo Fisher Scientific Inc.), following centrifugation of the protein fraction at 10,000 x g for at 4˚C for 15 min. Proteins (20-50 μg) were separated by 12% SDS-PAGE (w/v) and transferred onto PVDF membranes (EMD Millipore). The membranes were then blocked with 1% BSA for 2 h at room temperature, and incubated with the following primary antibodies overnight at 4˚C: TAK1 (cat no. 5206, 1:1,000), Bax (cat no. 5023, 1:1,000), Bcl-2 (cat no. 3498, 1:1,000), nuclear p-p65 (cat no. 3036, 1:1,000), p-IκB-α (cat no. 2859, 1:1,000), IκB-α (cat no. 4814, 1:1,000), histone H3 (cat no. 9728, 1:1,000) and β-actin (cat no. 4970, 1:1,000). Subsequently, the membranes were incubated with HRP-linked anti-rabbit IgG antibody (cat no. 7074, 1:2,000) and incubated with ECL reagent (GE Healthcare) for the detection of protein expression. All antibodies were obtained from Cell Signaling Technology, Inc. The gray value of the analyzed proteins was determined using the ImageJ software (version 1.46; Rawak Software Inc.).

Statistical analysis. GraphPad Prism 5.0 (GraphPad Software, Inc.) was used to perform the statistical analyses. Statistically significant differences were analyzed using an unpaired Student's t-test or one-way analysis of variance followed by Tukey's post hoc test. The correlation between TAK1 and miR-129 expression was analyzed using Pearson's correlation analysis. The differences in overall survival were assessed by Kaplan-Meier survival analysis and the log-rank test. All data are presented as the mean ± SD, and P<0.05 was considered to indicate a statistically significant difference.

Results

Downregulation of miR-129 in mice with ALI. The analysis of the expression of miRNAs included in the miRNA array expression profile dataset (GSE133733) from GEO revealed that there was a significant difference between the control group and the sepsis group (Fig. 1A). Out of the 38 miRNAs with a notable difference in relative expression levels, 21 were downregulated and 17 were upregulated in the sepsis group, compared with the control group: The expression of miR-129-5p (32), miR-27a (33), and miR-150 (34) was decreased, while the expression of miR-34b-5p (35), miR-155-3p (36) and miR-146-3p (37) was increased. This finding is consistent with previous reports and indicates the reliability of the microarray results in the present study. However, miR-129 was selected for further investigation as it exhibited the most statistically significant difference between the two groups and as previous studies have discussed the role of miR-129 in regulating injury and inflammatory response in different organ injury models (19,38,39).

To evaluate the therapeutic effects of miR-129, a model of LPS-induced lung injury was used, as previously described (40), as LPS administration is one of the most widely used murine experimental models for lung injury (41,42). As depicted in Fig. 1B, the administration of LPS alone resulted in the destruction of the lung architecture and in inflammation. The lung injury scores based on histopathological changes were significantly higher in the LPS group than in the control group,

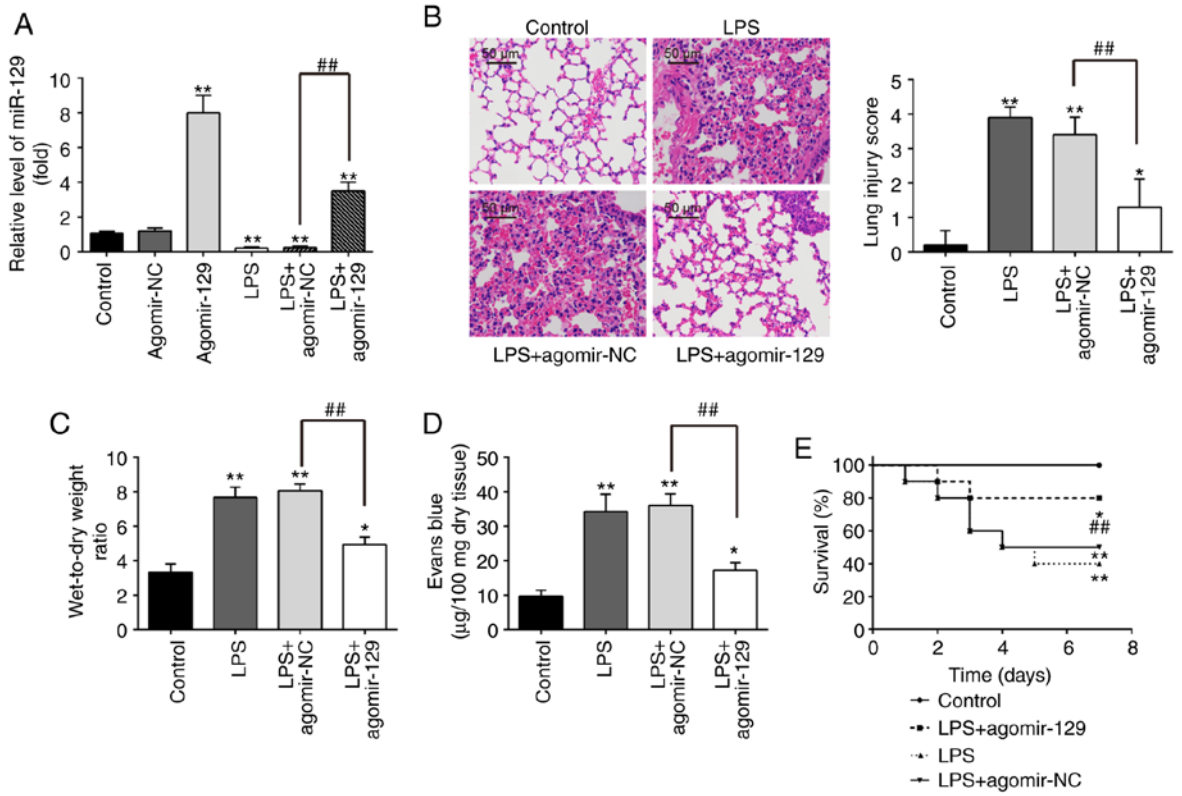

Figure 2. Amelioration of LPS-induced ALI in mice via the upregulation of miR-129. Mice were conducted by dripping 0.2 ml agomir-129 or agomir-NC (8 mg/kg) intravenously via tail vein before LPS stimulation. The mice were sacrificed 72 h after the LPS administration and lung tissues were then collected for analysis. (A) RT-qPCR analysis revealed that miR-129 was overexpressed in the mice treated with the agomir-129. (B) Lung tissues excised at 72 h after the LPS challenge; x200 magnification. (C) Assessment of lung permeability with the Evans blue dye extravasation method. (D) The lung wet/dry weight ratio was determined at 72 h after the LPS administration. Data represent the mean ± SD of three independent experiments. *P<0.05, **P<0.01 vs. the control group. $^{\#\#}$P<0.01 vs. the LPS + agomir-NC group. (E) The survival rates were observed during 7 days following exposure to LPS. *P<0.05 and **P<0.01 vs. the control group; $^{\#\#}$P<0.01 vs. the LPS + agomir-NC group. LPS, lipopolysaccharide; ALI, acute lung injury.

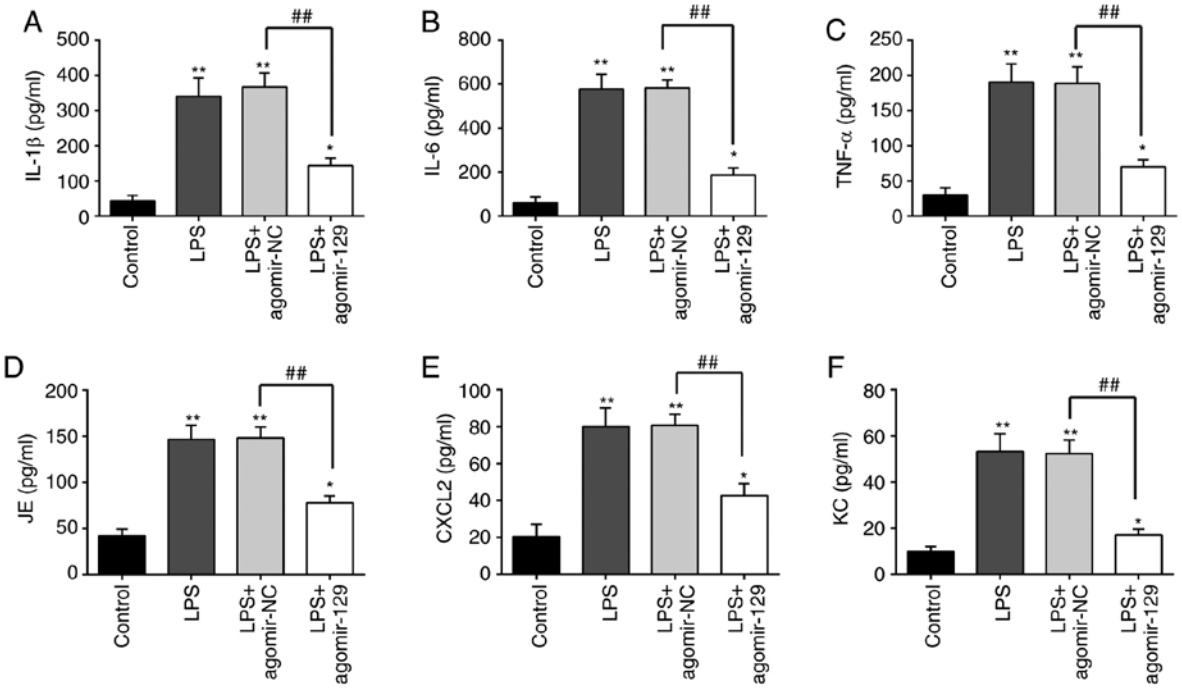

Figure 3. Attenuation of LPS-induced inflammation response in mice via the upregulation of miR-129. Mice were conducted by dripping agomir-129 or agomir-NC before LPS treatment. The mice were at sacrificed 72 h after the LPS administration, and BALF was then collected for analysis. (A-C) IL-1β, IL-6 and TNF-α levels in BALF measured at 72 h after the LPS challenge. (D-F) Levels of the chemokines JE, Cxcl2, and KC in BALF measured at 72 h after the LPS challenge Data represent the mean ± SD of three independent experiments. *P<0.05, **P<0.01 vs. the control group. $^{\#\#}$P<0.01 vs. the LPS + agomir-NC group. LPS, lipopolysaccharide; ALI, acute lung injury; BALF, bronchoalveolar lavage fluid.

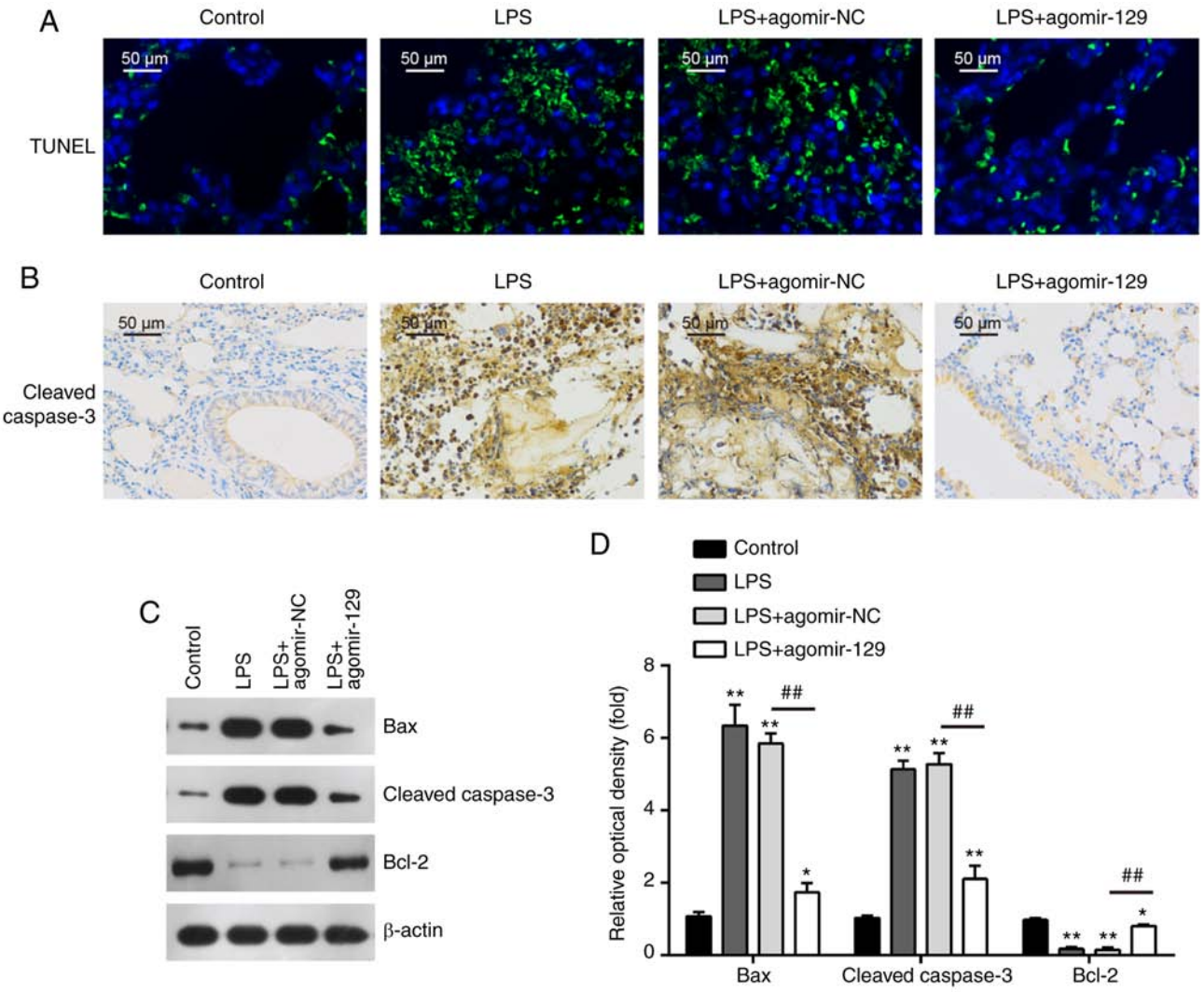

Figure 4. Inhibition of LPS-induced apoptosis via the overexpression of miR-129. Mice were treated by dripping agomir-129 or agomir-NC via tail vein before ALI was induced. The mice were sacrificed at 72 h after the LPS administration, and then the lung tissues were collected for analysis. (A) The apoptosis in the lung tissues was detected by TUNEL assay; x200 magnification. (B) The expression of cleaved-caspase 3 was determined by immunohistochemistry; x200 magnification. (C) The protein expression levels of Bcl-2, Bax and cleaved-caspase 3 were detected by western blot analysis. (D) The bands were semi-quantitatively analyzed using ImageJ software, normalized to β-actin density. Data represent the mean ± SD of three independent experiments. *P<0.05, **P<0.01 vs. the control group. $^{\#\#}$P<0.01 vs. the LPS + agomir-NC group. LPS, lipopolysaccharide; ALI, acute lung injury.

indicating that the ALI model was successfully established. At 72 h after the LPS challenge, lung tissue and BALF were harvested, and RT-qPCR was performed in order to measure the miR-129 expression levels. As was expected, miR-129 expression was notably decreased in response to the LPS challenge in BALF and lung tissues (Fig. 1C and D). These findings indicate that miR-129 may be involved in the development of ALI.

Alleviation of LPS-induced lung injury via miR-129 upregulation. Gain-function experiments were performed through the administration of agomiR-129, in order to investigate the potential protective effects of miR-129 against LPS-induced ALI. The expression levels of miR-129 in lung tissues was significantly elevated following the agomiR-129 injection in comparison with the control group expression levels (Fig. 2A), suggesting miR-129 overexpression has been successfully induced in mice, following agomiR-129 administration. Moreover, the miR-129 expression levels were significantly decreased in the LPS group as compared with the control group, whereas in the LPS + agomiR-129 group, the level of miR-129 was significantly increased compared with the LPS + agomiR-NC group (Fig. 2A). Histopathological analysis revealed that agomiR-129 administration attenuated the severity of lung injury caused by LPS, as indicated by the decrease in lung injury scores (Fig. 2B). The lung W/D ratio was calculated as an indicator of lung edema, which is an important feature of ALI (43). These results demonstrated that the lung W/D ratio was markedly increased by the LPS challenge, whereas it was significantly decreased following agomiR-129 administration in mice with LPS-induced ALI (Fig. 2C). In addition, the evaluation of lung microvascular permeability with the EB extravasation method revealed that the LPS challenge led to a significant increase in EB extravasation, which is considered as an indicator of lung vascular permeability, as compared with the control group EB extravasation (Fig. 2D). As was expected, agomiR-129 administration effectively reduced the LPS-induced increase in EB extravasation. Furthermore, agomiR-129 administration

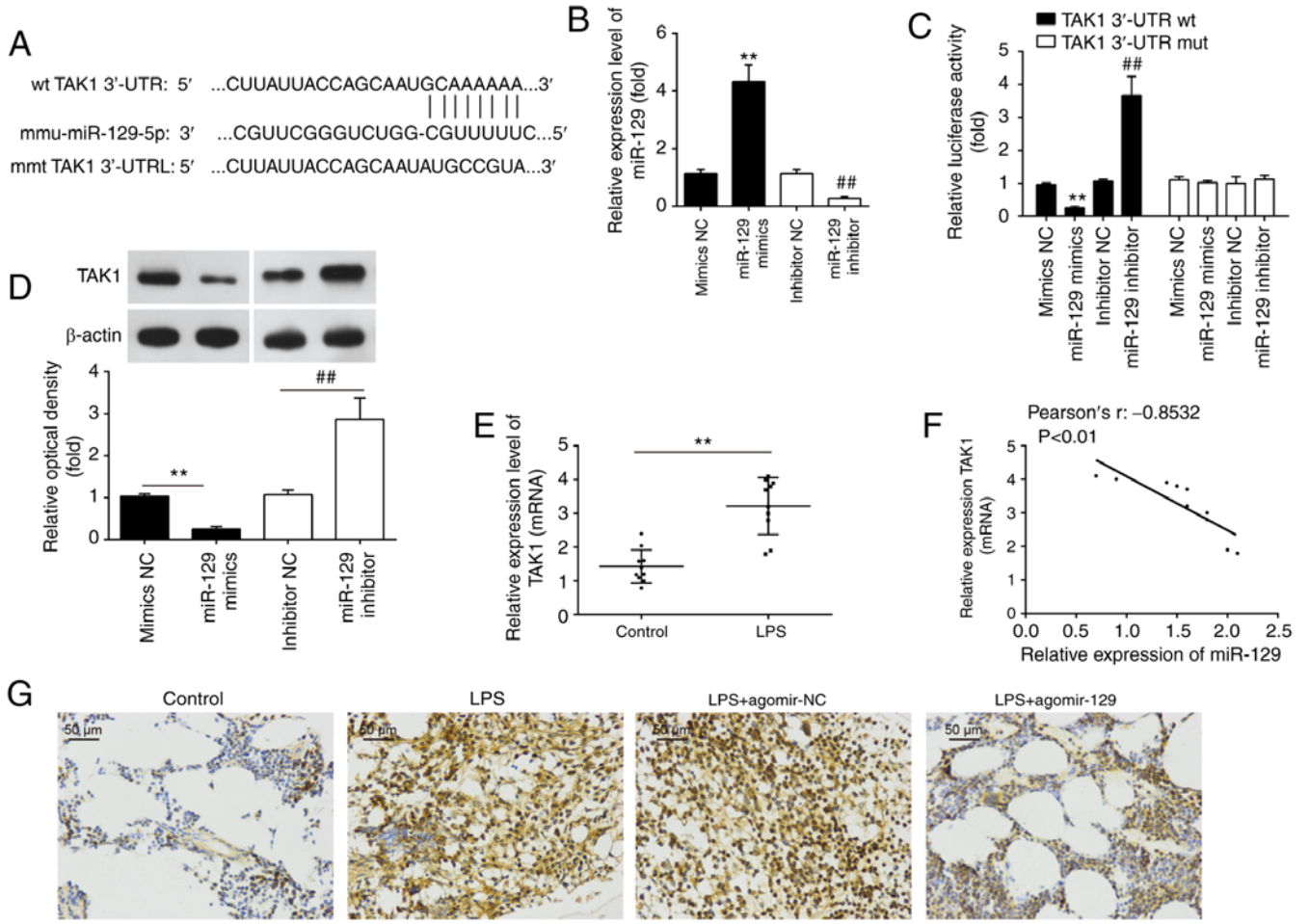

Figure 5. TAK1 is a direct target of miR-129. (A) The putative binding site of miR-129 and TAK1 is shown. (B) The expression levels of miR-129 were detected by RT-qPCR in RAW 264.7 cells following miR-129 mimic/inhibitor transfection. (C) Luciferase assay of RAW 264.7 cells, co-transfected with Firefly luciferase constructs, containing the TAK1 wild-type or mutated 3'-UTRs and miR-129 mimics, NC mimics, miR-129 inhibitor or NC inhibitor (n=3). Data represent the mean ± SD of three independent experiments. **P<0.01 vs. NC mimic, $^{\#\#}$P<0.01 vs. NC inhibitor. (D) Analysis of the expression of TAK1 mRNA and protein following transfection with miR-129 mimic or miR-129 inhibitor was measured by RT-qPCR and western blot analysis. Data represent the mean ± SD of three independent experiments. **P<0.01 vs. NC inhibitor. $^{\#\#}$P<0.01 vs. NC mimic. (E) RT-qPCR measurement of TAK1 expression in lungs from ALI mice. Data represent the mean ± SD of three independent experiments. **P<0.01 vs. the control group. (F) Pearson's correlation analysis revealed a negative correlation between the expression of TAK1 and miR-129 (r=-0.8532, P<0.01). (G) Immunohistochemistry of TAK1 expression in lung tissues; x200 magnification. TAK1, transforming growth factor activated kinase-1; LPS, lipopolysaccharide.

resulted in a significant increase in the survival rate (P<0.01; Fig. 2E). Taken together, these findings suggest that miR-129 may alleviate the pathological effects of ALI.

Alleviation of LPS-induced inflammation in BALF via miR-129 upregulation. The effects of miR-129 on the inflammatory response in ALI were then examined. The measurement of the levels of pro-inflammatory cytokines and chemokines in BALF from mice with ALI revealed that the concentrations of the inflammatory cytokines, IL-1β, IL-6 and TNF-α, and the chemokines, JE, Cxcl2 and KC, were markedly higher in the LPS group than in the control group. However, agomiR-129 administration inhibited the LPS-induced inflammatory cytokine and chemokine production (Fig. 3). These results indicate that miR-129 upregulation alleviates LPS-induced inflammatory response in ALI.

Alleviation of LPS-induced apoptosis by miR-129 upregulation. Since alveolar epithelial cells apoptosis is another important feature of ALI, lung tissue apoptosis was evaluated by TUNEL assay. The number of TUNEL-positive cells was markedly increased in the mouse lungs following LPS administration; however, the number of TUNEL-positive cells was markedly decreased in the lungs of the mice that were administered agomir-129 after the LPS administration (Fig. 4A). In addition, the relative levels of important proteins involved in apoptotic pathways were measured. Immunohistochemistry assay demonstrated that the expression levels of cleaved caspase-3 were markedly higher in the LPS group than in the control group, whereas agomiR-129 administration markedly inhibited the LPS-induced increase in caspase-3 expression levels (Fig. 4B). In addition, western blot analysis revealed that in comparison with the control group, the protein levels of the pro-apoptotic proteins, cleaved caspase-3 and Bax, were significantly increased, while the protein levels of the anti-apoptotic protein, Bcl-2, were decreased in the LPS group. AgomiR-129 administration markedly attenuated the effects of LPS on the apoptosis-related protein levels (Fig. 4C and D). Collectively, these results suggest that miR-129 upregulation inhibits LPS-induced lung cell apoptosis in mice.

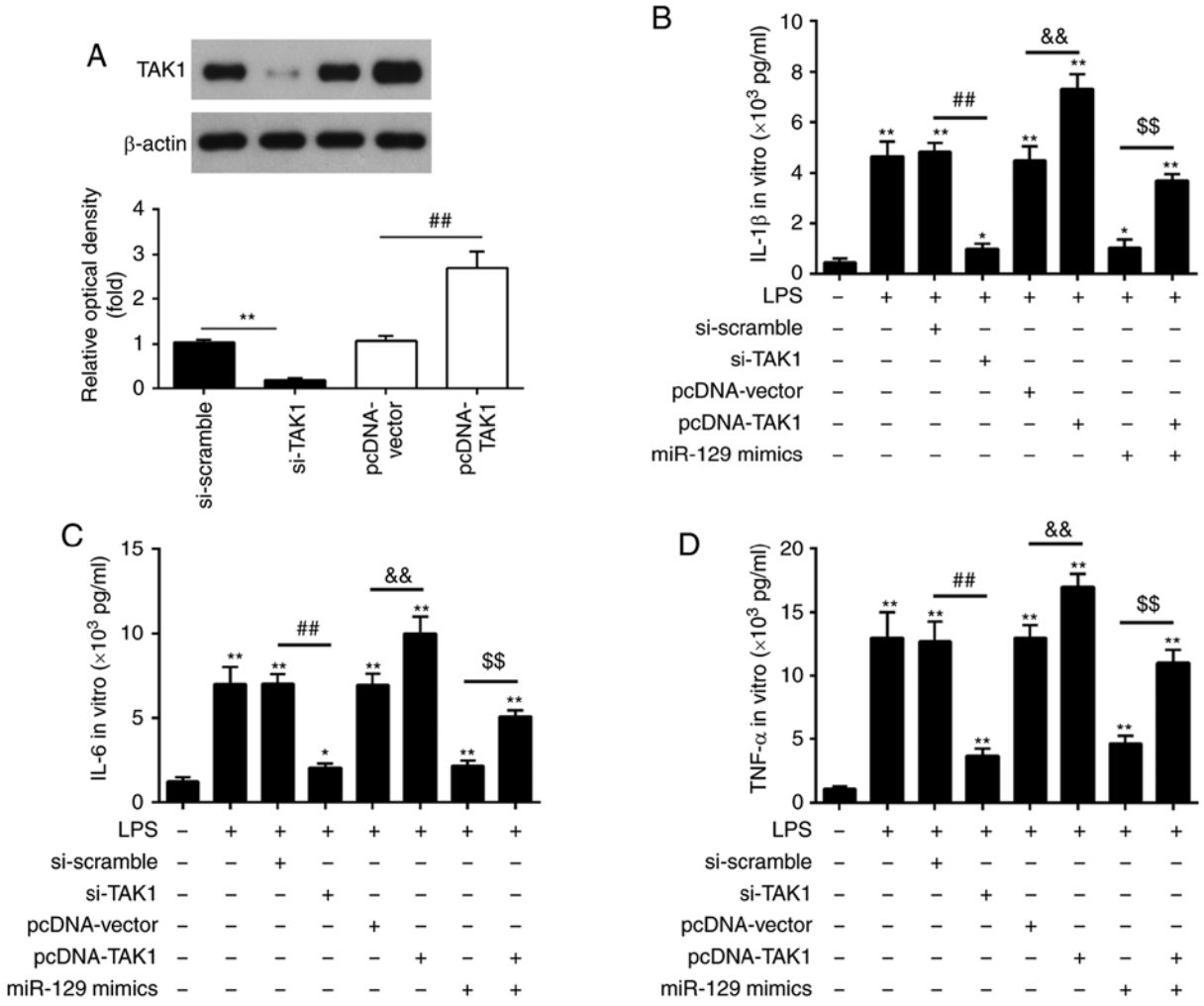

Figure 6. TAK1-mediated protective effect of miR-129 against LPS-induced apoptosis and inflammatory response in RAW264.7 cells. TAK1 expression vector, pcDNA-TAK1 or si-TAK1, together with miR-129 mimics were transfected into RAW264.7 cells 6 h prior to LPS treatment. (A) Western blot analysis of the protein expression levels of TAK1. Data represent the mean ± SD of three independent experiments. **P<0.01 vs. the si-scramble group. $^{\#\#}$P<0.01 vs. the pcDNA-vector group. (B-D) IL-1β, IL-6 and TNF-α levels in the cellular supernatant were measured using ELISA. Data represent the mean ± SD of three independent experiments. *P<0.05, **P<0.01 vs. the control group. $^{\#\#}$P<0.01 vs. the LPS + si-scramble group; $^{\&\&}$P<0.01 vs. the LPS + pcDNA-vector group; $^{\$\$}$P<0.01 vs. the LPS + miR-129 mimics group. TAK1, transforming growth factor activated kinase-1; LPS, lipopolysaccharide.

miR-129-induced inhibition of TAK1 under in vitro and in vivo conditions. In order to elucidate the molecular mechanisms instigating the miR-129 protective effects against LPS-induced apoptosis and the inflammatory response in mice with ALI, the potential target genes of miR-129 were analyzed using PicTar version 2007 (https://pictar.mdc-berlin.de/) and TargetScan Release 7.0 (http://targetscan.org/). Bioinformatics analysis indicated that TAK1 was a miR-129 potential target (Fig. 5A). To verify this association, a luciferase reporter assay was performed. To this end, the transfection efficiency of miR-129 mimics/inhibitor was first evaluated by RT-qPCR. The results revealed that miR-129 relative expression was significantly upregulated/downregulated as compared with the mir-NC group (Fig. 5B). Subsequently, it was found that the luciferase activity of wt-TAK1 3'UTR was significantly decreased after miR-129 mimics transfection and increased after the miR-129 inhibitor transfection. However, this effect was not observed, when mut-TAK1 3'UTR was used (Fig. 5C). It was also observed that miR-129 overexpression resulted in a decrease in TAK1 expression in RAW 264.7 cells, while miR-129 knockdown resulted in a significant increase in TAK1 protein expression levels (Fig. 5D).

In order to determine whether miR-129 also regulates TAK1 expression *in vivo*, TAK1 expression was detected in the lungs of mice with ALI. The results revealed that TAK1 expression was significantly increased following the LPS challenge (Fig. 5E). Furthermore, miR-129 expression was found to inversely correlate with TAK1 protein expression levels in lung tissues (Fig. 5F). As also observed *in vitro*, the increase in TAK1 protein expression due to LPS administration was markedly attenuated by the agomiR-129 administration (Fig. 5G). On the whole, these results indicate that TAK1 is a functional target of miR-129 in ALI.

TAK1-mediated protective effect of miR-129 against LPS-induced apoptosis and inflammatory response in RAW264.7 cells. Considering the important role of TAK1 in the inflammatory response following ALI, the present study attempted to determine whether TAK1 mediated the protective effects of miR-129 against ALI-associated inflammation (44).

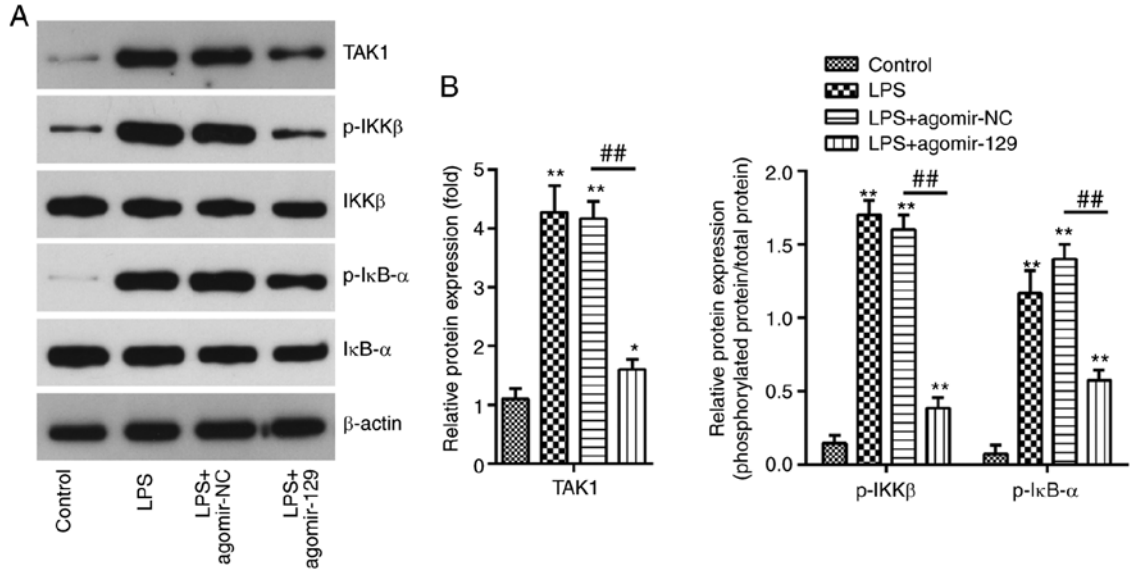

Figure 7. Blocking of the TAK1/NF-κB pathway in mice with LPS-induced ALI via overexpression of miR-129. Mice were conducted by injection agomir-129 or agomir-NC via tail vein before the ALI was induced. All mice were divided to four groups, Control, LPS, LPS + agomir-129 and LPS + agomir-NC. The mice were sacrificed after LPS administration for 72 h, and the lung tissues were then collected for analysis. (A) The levels of TAK1, p-IKKβ and p-IκB-α in four groups were measured by western blot analysis. (B) The bands were semi-quantitatively analyzed using the ImageJ software, normalized to β-actin density. Data represent the mean ± SD of three independent experiments. **P<0.01 vs. the control group. $^{\#\#}$P<0.01 vs. the LPS + agomir-NC group. TAK1, transforming growth factor activated kinase-1; LPS, lipopolysaccharide.

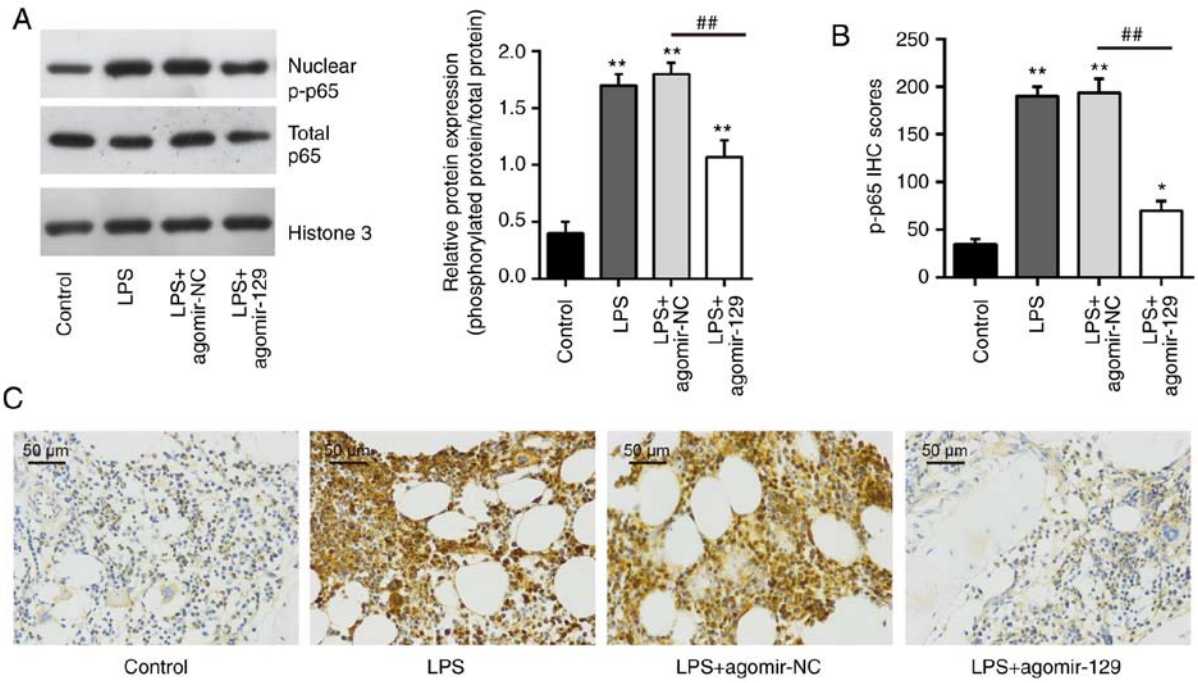

Figure 8. Inhibition of NF-κB pathway activation in mice with LPS-induced ALI via the overexpression of miR-129. (A) Expression of nuclear p-p65 was measured by western blot analysis in lung tissues. Data represent the mean ± SD of three independent experiments. **P<0.01 vs. the control group. $^{\#\#}$P<0.01 vs. the LPS + agomir-NC group. (B and C) Immunohistochemistry of the expression of nuclear p-p65 in lung tissue samples; x200 magnification. *P<0.05, **P<0.01 vs. the control group. $^{\#\#}$P<0.01 vs. the LPS + agomir-NC group.

A TAK1 expression vector, pcDNA-TAK1, or si-TAK1, together with miR-129 mimics, was transfected into RAW264.7 cells 6 h prior to LPS stimulation. The results demonstrated that pcDNA-TAK1 caused a significant increase in TAK1 protein expression levels, while si-TAK1 transfection resulted in a marked decrease in TAK1 protein expression levels (Fig. 6A). The production of the inflammatory cytokines, IL-1β, IL-6 and TNF-α was evaluated using ELISA in LPS-stimulated RAW264.7 cells co-transfected with pcDNA-TAK1 and miR-129 mimics or si-TAK1 and miR-129 mimics. As depicted in Fig. 6B-D, LPS stimulation significantly increased the secretion of IL-1β, IL-6 and TNF-α, which was suppressed by si-TAK1, whereas it was enhanced by TAK1 overexpression. In LPS-stimulated RAW264.7 cells, transfection with

si-scramble or pcDNA-vector alone had no significant effect on the inflammatory cytokine levels when compared with the LPS group. Notably, the inhibitory effects of miR-129 mimics on the production of the inflammatory cytokines were reversed by TAK1 overexpression in LPS-stimulated RAW264.7 cells Thus, these findings imply that miR-129 protects RAW264.7 cells from LPS-induced inflammatory response by targeting TAK1.

Inhibition of TAK1/NF-κB pathway activation by miR-129 upregulation. TAK1 has been shown to activate the NF-κB pathway (45), and the inhibition of the TAK1/NF-κB signaling pathway has been found to reduce the production of the pro-inflammatory cytokines, IL-1β, IL-6 and TNF-α (46). In the present study, in order to investigate the effects of miR-129 on TAK1/NF-κB pathway activation, the p-IKKβ, IKKβ, p-IκB-α, and IκB-α expression levels of were examined by western blot analysis. It was found that the TAK1, p-IKKβ and p-IκB-α protein expression levels were significantly increased after the LPS challenge, and that these effects were attenuated by agomiR-129 administration (Fig. 7). To confirm that miR-129 blocks the NF-κB pathway, the expression of nuclear p-p65 was examined by western blot analysis and immunohistochemistry. As was expected, the increased expression of nuclear p-p65 induced by LPS was reduced after agomiR-129 administration (Fig. 8). All these data indicate that miR-129 upregulation may block TAK1-mediated activation of the NF-κB pathway in mice with ALI.

Discussion

In the present study, the potential role of miR-129 in the pathogenic mechanisms of ALI was investigated. According to the results obtained, miR-129 was downregulated in lung tissues and BALF from mice with ALI; the subsequent upregulation of miR-129 alleviated LPS-induced ALI by suppressing pulmonary inflammation and apoptosis in mice. Additionally, it was demonstrated that TAK1 was a target of miR-129, that the miR-129 mimic agomiR-129 blocked LPS-induced TAK1 upregulation and, that it blocked activation of the NF-κB pathway. These findings suggest that miR-129 upregulation may be a promising therapeutic strategy for the prevention and treatment of ALI in future clinical trials.

A large body of evidence has revealed that miRNAs are aberrantly expressed in ALI, and may influence the pathophysiological mechanisms of ALI, such as inflammation and apoptosis (40,47). For example, Wang *et al* (26) demonstrated that miR-326 suppressed sepsis-induced inflammation and oxidative stress in macrophages via downregulation of TLR4. Additionally, Zhang *et al* (48) found that miR-146a upregulation alleviated inflammatory reaction and lung tissue injury in mice with sepsis-induced ALI, and Cao *et al* (49) demonstrated that miR-145 could ameliorate sepsis-induced lung injury by inhibiting the TGFBR2 signaling pathway. Thus, understanding the functions of miRNAs that are abnormally expressed in sepsis-induced ALI may help to improve therapeutic approaches for ALI. In the present study, the analysis of the microarray dataset (GSE133733) retrieved from GEO revealed that large numbers of miRNAs were significantly deregulated; in particular, miR-129 exhibited the highest level of downregulation. The ALI-associated decrease in its expression was confirmed by RT-qPCR analysis in lung tissue and BALF from mice with ALI. All these findings strongly indicate that miR-129 may be involved in sepsis-induced ALI.

The release of inflammatory factors and cell apoptosis in alveolar epithelial cells are considered be the underlying pathogenic mechanisms of ALI (50). In particular, the disruption of epithelial cell function and increased alveolar epithelial cell apoptosis have been observed in sepsis-induced ALI (51). Furthermore, apoptotic signaling pathways were found to be significantly more active in patients with ALI (52). In addition, the *in vivo* administration of apoptotic protease inhibitors has been found to reduce the mortality of mice with ALI (53). Therefore, the inhibition of apoptosis may be an effective strategy with which to decrease the incidence of ALI and ultimately provide a cure.

Previous studies have demonstrated that miR-129 plays protective roles in multiple injury models. For example, Yang *et al* (54) demonstrated that miR-129 overexpression improved neurological function by reducing tissue loss and cell apoptosis in a rat spinal cord injury model. Furthermore, Zeng *et al* (18) found that the upregulation of miR-129 reduced nerve injury and inflammatory response in rats with Alzheimer's disease via the downregulation of SOX6, and Ma *et al* (38) reported that miR-129 alleviated myocardial injury induced by I/R both under *in vitro* and *in vivo* conditions by targeting suppressor of cytokine signaling 2. Chen *et al* (19) also found that miR-129 played a protective role in myocardial I/R injury by regulating HMGB1 expression. Importantly, a recent study reported that the expression of miR-129 was decreased in mice with sepsis, and an enhanced miR-129 expression markedly improved sepsis-induced intestinal injury (55). However, the role of miR-129 in sepsis-induced lung injury has not yet been reported, at least to the best of our knowledge. In the present study, it was demonstrated that miR-129 upregulation markedly reduced the severity of lung injury and alleviated lung edema and lung permeability, accompanied by a significant reduction in the inflammatory response and apoptosis in mice with ALI. Taken together, the aforementioned findings indicate that the upregulation of miR-129 alleviated *in vivo* LPS-induced lung injury by suppressing inflammation and apoptosis. However, the underlying molecular mechanisms involved in miR-129-mediated inflammation and apoptosis suppression remain unclear.

TAK1, which is a member of the mitogen-activated protein kinase family, has received attention in inflammatory diseases including ALI (44,56). For instance, the inhibition of TAK1 was previously shown to mediate the potent protective effect of 4'-hydroxywogonin against LPS-induced in mice with ALI (57). Another study also mentioned that methyl salicylate 2-*O*-β-d-lactoside, a natural derivative of salicylate extracted from *Gaultheria yunnanensis*, exerted a therapeutic effect against LPS-induced ALI by inhibiting TAK1/NF-κB in mice (12). In the present study, bioinformatics analysis and luciferase assay indicated that TAK1 was a direct target of miR-129. More importantly, TAK1 was significantly upregulated and inversely correlated with miR-129 levels in lung tissues from ALI mice. Furthermore,

it was found that TAK1 overexpression reversed miR-129 inhibitory effects on LPS-induced inflammatory response and apoptosis in RAW264.7 cells, whereas TAK1 inhibition aggravated LPS-induced inflammatory response and apoptosis. All these data indicate that miR-129 upregulation improves LPS-induced inflammation and apoptosis through TAK1 targeting.

It is well known that NF-κB is a downstream signaling factor of TAK1 (45), and the TAK1/NF-κB axis has been demonstrated to play important roles in a variety of biological processes, such as inflammation (58). Of note, a previous study demonstrated that miR-129 ameliorated intestinal inflammation in trinitrobenzene sulphonic acid-induced colitis mice through inhibition of the NF-κB signaling pathway (59). Another study demonstrated that miR-129 improved neuronal injury of the hippocampus by suppressing the inflammation response via inhibition of the NF-kB signaling pathway (60). Given the interaction between TAK1 and miR-129, it was further determined whether miR-129 affects the NF-κB pathway by regulating TAK1 expression in sepsis-induced ALI. As was expected, miR-129 upregulation significantly decreased NF-κB pathway-related core factor (nuclear p-p65, p-IKKβ, and p-IκB-α) relative expression levels in ALI mice. These results indicate that miR-129 suppressed the inflammatory response and apoptosis in ALI through the TAK1/NF-κB signaling pathway.

miR-129 may also exert its protective effects in ALI via the regulation of other downstream targets. However, investigating additional miR-129 targets was beyond the scope of the present study, due to current laboratory limitations. Therefore, further future research is required in order to investigate and identify other alternative miR-129 targets taking part in ALI development. In addition, the present study investigated the roles of miR-129 and its underlying mechanisms *in vitro* and *in vivo* model of ALI; however, data from clinical trials are required to validate the preliminary *in vitro* and *in vivo* result obtained. Therefore, the functions of miR-129 warrant further investigation in clinical trials data in the future.

In conclusion, the present study demonstrated that miR-129 ameliorated sepsis-induced ALI, via the suppression of inflammatory response and apoptosis, by targeting the TAK1/NF-κB pathway. Thus, the miR-129/TAK1/NF-κB axis may serve as a potential therapeutic target for ALI and holds promise for its therapeutic management.

Acknowledgements

Not applicable.

Funding

The present study was supported by the 23456 Talent Project of Henan Provincial People's Hospital and Medical Service Capacity Improvement Project in Henan Provincial Medical Institutions.

Availability of data and materials

The datasets used and/or analyzed during the current study are available from the corresponding author on reasonable request.

Authors' contributions

WY, LX, XJ and SL performed the experiments, contributed to data analysis, and wrote the manuscript. WY, LX, XJ and SL analyzed the data. LW conceptualized the study design and contributed to data analysis and experimental materials. WY and LW confirm the authenticity of all the raw data. All authors have read and approved the final version of the manuscript.

Ethics approval and consent to participate

The animal experiments were approved by the Animal Care and Use Committee of Henan Provincial People's Hospital.

Patient consent for publication

Not applicable.

Competing interests

The authors declare that they have no competing interests.

References

1. Hoesel LM, Neff TA, Neff SB, Younger JG, Olle EW, Gao H, Pianko MJ, Bernacki KD, Sarma JV and Ward PA: Harmful and protective roles of neutrophils in sepsis. Shock 24: 40-47, 2005.
2. Villar J, Blanco J, Añón JM, Santos-Bouza A, Blanch L, Ambrós A, Gandía F, Carriedo D, Mosteiro F, Basaldúa S, *et al*: The ALIEN study: Incidence and outcome of acute respiratory distress syndrome in the era of lung protective ventilation. Intensive Care Med 37: 1932-1941, 2011.
3. Gill SE, Taneja R, Rohan M, Wang L and Mehta S: Pulmonary microvascular albumin leak is associated with endothelial cell death in murine sepsis-induced lung injury in vivo. PLoS One 9: e88501, 2014.
4. Jiang C, Ting AT and Seed B: PPAR-gamma agonists inhibit production of monocyte inflammatory cytokines. Nature 391: 82-86, 1998.
5. Strieter RM, Belperio JA and Keane MP: Cytokines in innate host defense in the lung. J Clin Invest 109: 699-705, 2002.
6. Hoesel B and Schmid JA: The complexity of NF-κB signaling in inflammation and cancer. Mol Cancer 12: 86, 2013.
7. Jiang T, Tian F, Zheng H, Whitman SA, Lin Y, Zhang Z, Zhang N and Zhang DD: Nrf2 suppresses lupus nephritis through inhibition of oxidative injury and the NF-κB-mediated inflammatory response. Kidney Int 85: 333-343, 2014.
8. Gross CM, Kellner M, Wang T, Lu Q, Sun X, Zemskov EA, Noonepalle S, Kangath A, Kumar S, Gonzalez-Garay M, *et al*: LPS-induced acute lung injury involves NF-κB-mediated downregulation of SOX18. Am J Respir Cell Mol Biol 58: 614-624, 2018.
9. Yang H, Lv H, Li H, Ci X and Peng L: Oridonin protects LPS-induced acute lung injury by modulating Nrf2-mediated oxidative stress and Nrf2-independent NLRP3 and NF-κB pathways. Cell Commun Signal 17: 62, 2019.
10. Yang KY, Arcaroli JJ and Abraham E: Early alterations in neutrophil activation are associated with outcome in acute lung injury. Am J Respir Crit Care Med 167: 1567-1574, 2003.
11. Schwartz MD, Moore EE, Moore FA, Shenkar R, Moine P, Haenel JB and Abraham E: Nuclear factor-kappa B is activated in alveolar macrophages from patients with acute respiratory distress syndrome. Crit Care Med 24: 1285-1292, 1996.
12. Yang S, Yu Z, Yuan T, Wang L, Wang X, Yang H, Sun L, Wang Y and Du G: Therapeutic effect of methyl salicylate 2-O-β-d-lactoside on LPS-induced acute lung injury by inhibiting TAK1/NF-kappaB phosphorylation and NLRP3 expression. Int Immunopharmacol 40: 219-228, 2016.
13. Bartel DP: MicroRNAs: Target recognition and regulatory functions. Cell 136: 215-233, 2009.
14. Guo Z, Gu Y, Wang C, Zhang J, Shan S, Gu X, Wang K, Han Y and Ren T: Enforced expression of miR-125b attenuates LPS-induced acute lung injury. Immunol Lett 162: 18-26, 2014.

15. Zhang Y, Xie Y, Zhang L and Zhao H: MicroRNA-155 participates in smoke-inhalation-induced acute lung injury through inhibition of SOCS-1. Molecules 25: 1022, 2020.
16. Wan G, An Y, Tao J, Wang Y, Zhou Q, Yang R and Liang Q: MicroRNA-129-5p alleviates spinal cord injury in mice via suppressing the apoptosis and inflammatory response through HMGB1/TLR4/NF-κB pathway. Biosci Rep 40: BSR20193315, 2020.
17. Li XQ, Chen FS, Tan WF, Fang B, Zhang ZL and Ma H: Elevated microRNA-129-5p level ameliorates neuroinflammation and blood-spinal cord barrier damage after ischemia-reperfusion by inhibiting HMGB1 and the TLR3-cytokine pathway. J Neuroinflammation 14: 205, 2017.
18. Zeng Z, Liu Y, Zheng W, Liu L, Yin H, Zhang S, Bai H, Hua L, Wang S, Wang Z, *et al*: MicroRNA-129-5p alleviates nerve injury and inflammatory response of Alzheimer's disease via downregulating SOX6. Cell cycle 18: 3095-3110, 2019.
19. Chen ZX, He D, Mo QW, Xie LP, Liang JR, Liu L and Fu WJ: MiR-129-5p protects against myocardial ischemia-reperfusion injury via targeting HMGB1. Eur Rev Med Pharmacol Sci 24: 4440-4450, 2020.
20. Xu Z, Zhang C, Cheng L, Hu M, Tao H and Song L: The microRNA miR-17 regulates lung FoxA1 expression during lipopolysaccharide-induced acute lung injury. Biochem Biophys Res Commun 445: 48-53, 2014.
21. Carbone L, Carbone ET, Yi EM, Bauer DB, Lindstrom KA, Parker JM, Austin JA, Seo Y, Gandhi AD and Wilkerson JD: Assessing cervical dislocation as a humane euthanasia method in mice. J Am Assoc Lab Anim Sci 51: 352-356, 2012.
22. Li C, Yang D, Cao X, Wang F, Jiang H, Guo H, Du L, Guo Q and Yin X: LFG-500, a newly synthesized flavonoid, attenuates lipopolysaccharide-induced acute lung injury and inflammation in mice. Biochem Pharmacol 113: 57-69, 2016.
23. Lei C, Jiao Y, He B, Wang G, Wang Q and Wang J: RIP140 down-regulation alleviates acute lung injury via the inhibition of LPS-induced PPARγ promoter methylation. Pulm Pharmacol Ther 37: 57-64, 2016.
24. Ayaz G, Halici Z, Albayrak A, Karakus E and Cadirci E: Evaluation of 5-HT7 receptor trafficking on in vivo and in vitro model of lipopolysaccharide (LPS)-induced inflammatory cell injury in rats and LPS-treated A549 cells. Biochem Genet 55: 34-47, 2017.
25. Shao L, Meng D, Yang F, Song H and Tang D: Irisin-mediated protective effect on LPS-induced acute lung injury via suppressing inflammation and apoptosis of alveolar epithelial cells. Biochem Biophys Res Commun 487: 194-200, 2017.
26. Wang Z, Yan J, Yang F, Wang D, Lu Y and Liu L: MicroRNA-326 prevents sepsis-induced acute lung injury via targeting TLR4. Free Radic Res 54: 408-418, 2020.
27. Bian B, Yu XF, Wang GQ and Teng TM: Role of miRNA-1 in regulating connexin 43 in ischemia-reperfusion heart injury: A rat model. Cardiovasc Pathol 27: 37-42, 2017.
28. Livak KJ and Schmittgen TD: Analysis of relative gene expression data using real-time quantitative PCR and the 2(-Delta Delta C(T)) method. Methods 25: 402-408, 2001.
29. Moitra J, Sammani S and Garcia JG: Re-evaluation of evans blue dye as a marker of albumin clearance in murine models of acute lung injury. Transl Res 150: 253-265, 2007.
30. Villar J, Cabrera-Benitez NE, Valladares F, García-Hernández S, Ramos-Nuez Á, Martín-Barrasa JL, Muros M, Kacmarek RM and Slutsky AS: Tryptase is involved in the development of early ventilator-induced pulmonary fibrosis in sepsis-induced lung injury. Crit Care 19: 138, 2015.
31. Varghese F, Bukhari AB, Malhotra R and De A: IHC Profiler: An open source plugin for the quantitative evaluation and automated scoring of immunohistochemistry images of human tissue samples. PLoS One 9: e96801, 2014.
32. Wu G, Li X, Li M and Zhang Z: Long non-coding RNA MALAT1 promotes the proliferation and migration of Schwann cells by elevating BDNF through sponging miR-129-5p. Exp Cell Res 390: 111937, 2020.
33. Ju M, Liu B, He H, Gu Z, Liu Y, Su Y, Zhu D, Cang J and Luo Z: MicroRNA-27a alleviates LPS-induced acute lung injury in mice via inhibiting inflammation and apoptosis through modulating TLR4/MyD88/NF-κB pathway. Cell Cycle 17: 2001-2018, 2018.
34. Li P, Yao Y, Ma Y and Chen Y: MiR-150 attenuates LPS-induced acute lung injury via targeting AKT3. Int Immunopharmacol 75: 105794, 2019.
35. Xie W, Lu Q, Wang K, Lu J, Gu X, Zhu D, Liu F and Guo Z: miR-34b-5p inhibition attenuates lung inflammation and apoptosis in an LPS-induced acute lung injury mouse model by targeting progranulin. J Cell Physiol 233: 6615-6631, 2018.
36. Yan Y, Lou Y and Kong J: MiR-155 expressed in bone marrow-derived lymphocytes promoted lipopolysaccharide-induced acute lung injury through Ang-2-Tie-2 pathway. Biochem Biophys Res Commun 510: 352-357, 2019.
37. Vaporidi K, Vergadi E, Kaniaris E, Hatziapostolou M, Lagoudaki E, Georgopoulos D, Zapol WM, Bloch KD and Iliopoulos D: Pulmonary microRNA profiling in a mouse model of ventilator-induced lung injury. Am J Physiol Lung Cell Mol Physiol 303: L199-L207, 2012.
38. Ma R, Chen X, Ma Y, Bai G and Li DS: MiR-129-5p alleviates myocardial injury by targeting suppressor of cytokine signaling 2 after ischemia/reperfusion. Kaohsiung J Med Sci 36: 599-606, 2020.
39. Huang X, Hou X, Chuan L, Wei S, Wang J, Yang X and Ru J: miR-129-5p alleviates LPS-induced acute kidney injury via targeting HMGB1/TLRs/NF-kappaB pathway. Int Immunopharmacol 89: 107016, 2020.
40. Fang Y, Gao F, Hao J and Liu Z: microRNA-1246 mediates lipopolysaccharide-induced pulmonary endothelial cell apoptosis and acute lung injury by targeting angiotensin-converting enzyme 2. Am J Transl Res 9: 1287-1296, 2017.
41. Tianzhu Z and Shumin W: Esculin inhibits the inflammation of LPS-induced acute lung injury in mice via regulation of TLR/NF-κB pathways. Inflammation 38: 1529-1536, 2015.
42. Mei SH, McCarter SD, Deng Y, Parker CH, Liles WC and Stewart DJ: Prevention of LPS-induced acute lung injury in mice by mesenchymal stem cells overexpressing angiopoietin 1. PLoS Med 4: e269, 2007.
43. Cheng KT, Xiong S, Ye Z, Hong Z, Di A, Tsang KM, Gao X, An S, Mittal M, Vogel SM, *et al*: Caspase-11-mediated endothelial pyroptosis underlies endotoxemia-induced lung injury. J Clin Invest 127: 4124-4135, 2017.
44. Liu H, Lin Z and Ma Y: Suppression of Fpr2 expression protects against endotoxin-induced acute lung injury by interacting with Nrf2-regulated TAK1 activation. Biomed Pharmacother 125: 109943, 2020.
45. Gao D, Wang R, Li B, Yang Y, Zhai Z and Chen DY: WDR34 is a novel TAK1-associated suppressor of the IL-1R/TLR3/TLR4-induced NF-kappaB activation pathway. Cell Mol Life Sci 66: 2573-2584, 2009.
46. Chen Q, Wu S, Wu Y, Chen L and Pang Q: MiR-149 suppresses the inflammatory response of chondrocytes in osteoarthritis by down-regulating the activation of TAK1/NF-κB. Biomed Pharmacother 101: 763-768, 2018.
47. Nan CC, Zhang N, Cheung KCP, Zhang HD, Li W, Hong CY, Chen HS, Liu XY, Li N and Cheng L: Knockdown of lncRNA MALAT1 alleviates LPS-induced acute lung injury via inhibiting apoptosis through the miR-194-5p/FOXP2 axis. Front Cell Dev Biol 8: 586869, 2020.
48. Zhang J, Ding C, Shao Q, Liu F, Zeng Z, Nie C and Qian K: The protective effects of transfected microRNA-146a on mice with sepsis-induced acute lung injury in vivo. Zhonghua Wei Zhong Bing Ji Jiu Yi Xue 27: 591-594, 2015 (In Chinese).
49. Cao X, Zhang C, Zhang X, Chen Y and Zhang H: MiR-145 negatively regulates TGFBR2 signaling responsible for sepsis-induced acute lung injury. Biomed Pharmacother 111: 852-858, 2019.
50. Li L, Wu W, Huang W, Hu G, Yuan W and Li W: NF-κB RNAi decreases the Bax/Bcl-2 ratio and inhibits TNF-α-induced apoptosis in human alveolar epithelial cells. Inflamm Res 62: 387-397, 2013.
51. Gong Y, Lan H, Yu Z, Wang M, Wang S, Chen Y, Rao H, Li J, Sheng Z and Shao J: Blockage of glycolysis by targeting PFKFB3 alleviates sepsis-related acute lung injury via suppressing inflammation and apoptosis of alveolar epithelial cells. Biochem Biophys Res Commun 491: 522-529, 2017.
52. Albertine KH, Soulier MF, Wang Z, Ishizaka A, Hashimoto S, Zimmerman GA, Matthay MA and Ware LB: Fas and fas ligand are up-regulated in pulmonary edema fluid and lung tissue of patients with acute lung injury and the acute respiratory distress syndrome. Am J Pathol 161: 1783-1796, 2002.
53. Kawasaki M, Kuwano K, Hagimoto N, Matsuba T, Kunitake R, Tanaka T, Maeyama T and Hara N: Protection from lethal apoptosis in lipopolysaccharide-induced acute lung injury in mice by a caspase inhibitor. Am J Pathol 157: 597-603, 2000.
54. Yang R, Cai X, Li J, Liu F and Sun T: Protective effects of MiR-129-5p on acute spinal cord injury rats. Med Sci Monit 25: 8281-8288, 2019.

55. Du X, Tian D, Wei J, Yan C, Hu P, Wu X and Yang W: MEG3 alleviated LPS-induced intestinal injury in sepsis by modulating miR-129-5p and surfactant protein D. Mediators Inflamm 2020: 8232734, 2020.
56. Chen Z, Zhang D, Li M and Wang B: Costunolide ameliorates lipoteichoic acid-induced acute lung injury via attenuating MAPK signaling pathway. Int Immunopharmacol 61: 283-289, 2018.
57. Fan C, Wu LH, Zhang GF, Xu F, Zhang S, Zhang X, Sun L, Yu Y, Zhang Y and Ye RD: 4'-Hydroxywogonin suppresses lipopolysaccharide-induced inflammatory responses in RAW 264.7 macrophages and acute lung injury mice. PLoS One 12: e0181191, 2017.
58. Cai PC, Shi L, Liu VW, Tang HW, Liu IJ, Leung TH, Chan KK, Yam JW, Yao KM, Ngan HY and Chan DW: Elevated TAK1 augments tumor growth and metastatic capacities of ovarian cancer cells through activation of NF-κB signaling. Oncotarget 5: 7549-7562, 2014.
59. Meng Q, Wu W, Pei T, Xue J, Xiao P, Sun L, Li L and Liang D: miRNA-129/FBW7/NF-κB, a novel regulatory pathway in inflammatory bowel disease. Mol Ther Nucleic Acids 19: 731-740, 2020.
60. Liu AH, Wu YT and Wang YP: MicroRNA-129-5p inhibits the development of autoimmune encephalomyelitis-related epilepsy by targeting HMGB1 through the TLR4/NF-kB signaling pathway. Brain Res Bull 132: 139-149, 2017.